Legless Locomotion for Legged Robots

Ravi Balasubramanian, Alfred A. Rizzi, and Matthew T. Mason
{bravi, arizzi, matt.mason}@cs.cmu.edu
The Robotics Institute, Carnegie Mellon University,
Pittsburgh, PA 15213, USA.

***Abstract*— We propose a locomotion technique for a legged robot that is *high-centered*, i.e., a robot stuck on a block with its legs dangling in air. By using its legs as reaction masses, the robot might be able to rock and roll on its stomach and incrementally move forward off the block, a form of legless locomotion using halteres. With locomotion of high-centered robots using body attitude oscillations as motivation, this paper focuses on studying the interplay between leg motions and body roll-pitch-yaw dynamics. We present results from simulation of two simplified models in which body motion is restricted to the roll and roll-yaw space respectively.**

I. INTRODUCTION

Legged robots offer good rough terrain mobility, but conventional legged locomotion fails when no leg can engage the ground (the robot is high-centered). The goal of this paper is to explore some unconventional modes of locomotion when legged robots are high-centered.

Our interest in this problem arose from experience with RHex [10], a simple and highly mobile hexapod robot (see Fig. 1). Each leg has a single actuated hip joint, which can rotate all the way around. When RHex is high-centered, no contact between legs and ground is possible. The only possible means of locomotion is by wiggling the legs and using them as reaction mass.

In at least one case, moving a high-centered RHex might be feasible even with small forces. Suppose there is a single rolling contact between robot and obstacle because the robot's stomach is rounded. Then, even small torques can cause the robot's attitude to oscillate, and these oscillations can generate translations due to nonholonomic contact constraints [8] between the body and obstacle.

To study the idea of locomotion by body attitude oscillations, we have constructed a simple prototype called the *RRRobot* (Rocking and Rolling Robot) which locomotes on its spherical stomach (see Fig. 2). Since its teleoperated legs act only as reaction masses, they are more properly called *halteres*, after the dumbbells sometimes used by athletes to give impetus in leaping. Table I gives a sequence of interleaved body roll and yaw motions that locomotes RRRobot in the XY-plane (see Fig. 3). In informal experiments, when we drove the halteres with periodic waveforms, the resulting motion included large oscillations in pitch and roll, some changes in yaw, and incremental translation. Our experiments with RRRobot suggest that oscillations in body attitude might be a practical way to recover from the high-centered state.

With locomotion of high-centered robots using attitude oscillations as motivation, the remainder of this paper focuses on the use of halteres to control the attitude of the body. We will consider only small attitude changes and assume that RRRobot translation

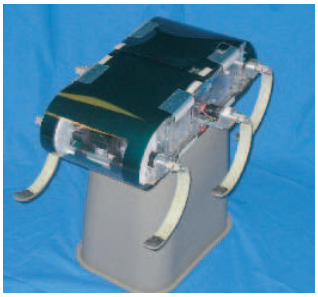

Fig. 1. The RHex experimental platform high-centered on a block (http://rhex.net).

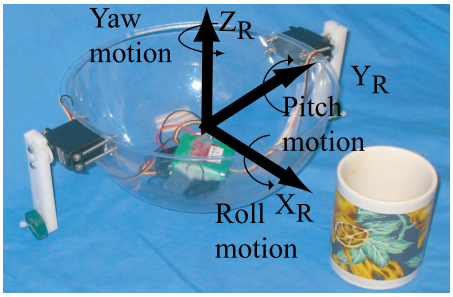

Fig. 2. The RRRobot experimental platform uses halteres to induce body attitude oscillations leading to body translations.

TABLE I

A sequence of roll-yaw motions that translates RRRobot in XY-plane (see Fig. 3).

Body motion	XY motion
Positive roll	P_0 to P_1
Positive yaw	P_1 to P_2
Negative roll	P_2 to P_3
Negative yaw	P_3 to P_4

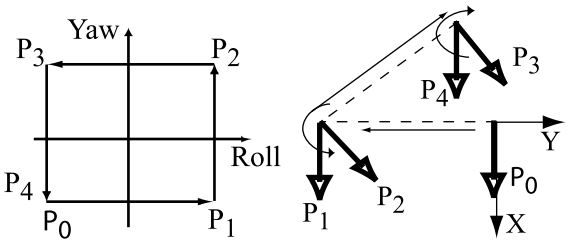

(a) (b)

Fig. 3. (a) Attitude oscillations in roll-yaw space and (b) corresponding translation in the XY-plane (see Table I).

has no effect on the body roll-pitch-yaw dynamics. Thus, we will fix the body center for the roll-pitch-yaw dynamics analysis. After a review of related work in Section 2, the body of the paper will explore two simplified models, one in which the body motion is limited to yaw (Section 2) and one in which the body motion is limited to roll and yaw (Section 3). Section 4 presents a brief discussion of how attitude oscillations, when coupled with kinematic contact constraints, can lead to RRRobot translation.

A. Related Work

The locomotion strategy we propose for RRRobot involves the interplay between roll-pitch-yaw dynamics and the nonholonomic kinematic contact constraints. Lewis et al. [5] discuss the constrained mechanics of the *Snakeboard*, a variation of the typical skateboard with a rotor and wheel directions as controls. Lewis et al. produce locomotion by using sinusoidal trajectories for the controls, while taking advantage of the contact constraints. In studying the RRRobot dynamics, we will use the Lagrangian method [4], which is easy to set up since it involves only computing the Lagrangian and taking its derivatives.

RRRobot locomotion depends on the kinematic rolling constraints determined by the curvatures of the two surfaces, the type of contact between the two surfaces, etc. [7]. Given the geometry of the two bodies, Li et al. [6] use Chow's theorem [3] to establish the existence of a path between any two configurations. Camicia et al. [2] provide an analysis of the nonholonomic kinematics and dynamics of the *Sphericle* [1], a hollow ball driven on a planar surface by an unicycle placed inside. The Sphericle and RRRobot have similar kinematic nonholonomic contact constraints.

Our approach to body attitude control using halteres is analogous to spinning reaction wheels to orient satellites. Rui et al. [9] present a controllability analysis and motion planning approaches for spacecraft attitude maneuvers using reaction wheels. But the main difference in our problem is that the roll and yaw inertias of RRRobot change with leg position, while in the case of satellites, the inertias of the system do not change with the rotation of reaction wheels. See Section II-C for more details.

In the rest of this report, we will focus on how flailing the legs affect body configuration in simplified RRRobot models.

II. The Yaw Model

We begin studying the roll-pitch-yaw dynamics by exploring a simplified RRRobot model that only yaws (see Fig. 4). The body center B is fixed, and there is no gravitational field. Body yaw configuration is represented by θ_2, and body roll and pitch are fixed at zero. Leg 1 joint angle is represented by ϕ_1, leg 2 joint angle by ϕ_2, and there are no joint limits. The masses, represented by black dots in Fig. 4, include three arranged symmetrically on the body and one at the distal end of each leg. Each body mass has value m_m, and each leg mass has value m_l. Torques τ_1 and τ_2 can be applied at leg joints 1 and 2, and all links are rigid.

A. Yaw model mathematical details

The yaw model equations of motion take the form

$$M(q)\ddot{q}+C(q,\dot{q})\dot{q} \;=\; \begin{pmatrix} 0 \\ \tau_1 \\ \tau_2 \end{pmatrix} \qquad (1)$$

where $q=(\theta_2,\phi_1,\phi_2)^T \in \mathbb{R}^3$ represents the configuration of the robot, $M(q)$ is the positive definite mass matrix, and $C(q,\dot{q})\dot{q}$ is the vector of velocity dependent force terms. Row 1 of (1) implies that body yaw is not directly actuated and is influenced by leg motions only. Trivially, we infer that if the leg

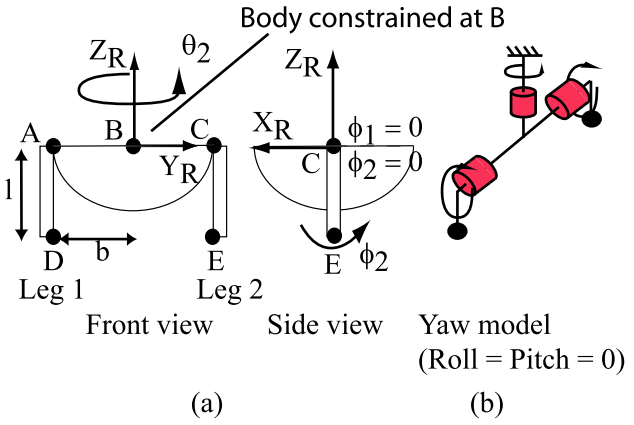

Fig. 4. (a) A simplified RRRobot model and (b) the yaw model as a kinematic chain.

velocities and accelerations are zero, then the body yaw velocity and acceleration must also be zero.

Equation (1) can be rewritten as

$$\dot{x} \quad = \quad f(x) + g_1(x) \cdot \tau_1 + g_2(x) \cdot \tau_2, \qquad (2)$$

where $f(x) = \begin{pmatrix} (\dot{q}, \\ -\bar{M}(q)C(q,\dot{q})\dot{q}) \end{pmatrix}$,
$g_1(x) = (0,0,0,\bar{M}_2(q))^T$, and
$g_2(x) = (0,0,0,\bar{M}_3(q))^T$.
Here, $x = (q,\dot{q})^T \in \mathbb{R}^6$ represents the state of the system, viz., the yaw model configuration and velocity, and $\dot{x} = (\dot{q},\ddot{q})^T \in \mathbb{R}^6$ represents the rate of change of the state of the system, viz., the yaw model velocity and acceleration. The matrix $\bar{M}(q)$ is the inverse of $M(q)$, and $\bar{M}_i(q)$ represents the i^{th} column of $\bar{M}$.

B. Yaw model formal analysis

In the control systems literature, (2) is said to be in state-space form. The vectors g_1 and g_2 are called control vector fields, corresponding to the controls τ_1 and τ_2, and f is called the drift vector field. We explore the yaw model by studying the vector fields f, g_1, and g_2 and their filtration [11], defined as the sequence $\{G_i\}$, such that

$$\begin{aligned} G_1 &= \text{Span}\{f, g_1, g_2\}, \\ G_i &= G_{i-1} + \text{Span}\{[G_1, G_{i-1}]\}, i > 1, \end{aligned}$$

where $[G_i, G_j]$ represents the Lie bracket between two distributions G_i and G_j. We list some observations of the yaw model.

1. The Lie bracket $[g_1, g_2]$ is identically zero. But the Lie brackets $[g_i, f]$ are non-zero and give new directions in the tangent space. Thus, the interaction between the control and drift vector fields is important for yaw model motion.

2. Rank(G_2) is 5, and the constraint direction on distribution G_2, i.e., the vector not in the span of G_2, is

$$N(x) = \begin{pmatrix} 0 \\ -\frac{l}{b}\dot{\theta}\sin 2\phi_1 - \dot{\phi}_1 \sin 2\phi_1 \\ -\frac{l}{b}\dot{\theta}\sin 2\phi_2 + \dot{\phi}_2 \sin 2\phi_2 \\ A(\phi_1, \phi_2) \\ \sin\phi_1 \\ -\sin\phi_2 \end{pmatrix}, \qquad (3)$$

where $A(\phi_1,\phi_2) = (m_l l^2(\cos 2\phi_1 + \cos 2\phi_2) + 2m_l l^2 + 4b^2(m_l + m_m))/(2m_l lb)$.

Note that $A(\phi_1,\phi_2)$ is never zero, implying that the constraint direction always has a component along the yaw acceleration direction.

3. It can be shown that all the second degree Lie brackets in G_3 (e.g., $[f,[g_1,f]]$) are perpendicular to $N(x)$. Thus, G_2 spans the second degree Lie brackets, and the spans of G_2 and G_3 are the same. Thus, we can do all analysis of the yaw model using distribution G_2 only.

4. From 3, we deduce that G_2 spans the tangent space of the yaw model T_x. Since $\dot{x} \in T_x$, $N(x) \cdot \dot{x} = 0$. Note that this equation is in Pfaffian form [8] and, when expanded, is identical to row 1 in (1).

Interestingly, since the dimension of the filtration is never greater than five, and the yaw system is embedded in a six-dimensional space, we conclude that the yaw system has a global holonomic constraint. For example, when the legs are horizontal ($\phi_1 = \phi_2 = 0$), using (3), we compute

$$N(x) = \begin{pmatrix} 0 \\ 0 \\ 0 \\ (2ml^2 + 2b^2(m_l + m_m))/(m_l lb) \\ 0 \\ 0 \end{pmatrix}.$$

Since the only non-zero element in $N(x)$ at this configuration is along the yaw acceleration direction, we infer that yaw velocity is fixed when the legs are horizontal.

C. Changing body yaw using leg motions

The goal of studying the yaw model is to explore the use of leg motions to affect body yaw. The yaw model is so simple that we can understand its motion

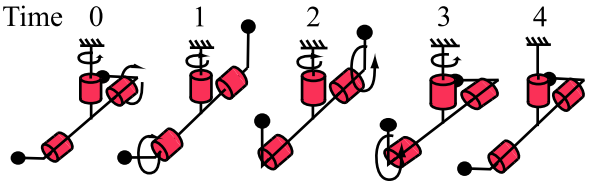

Fig. 5. Incremental motion of the yaw model using Lie bracket-inspired leg motions.

using the law of conservation of angular momentum. Suppose the system is at rest at $t = 0$, and the yaw angular momentum of the system about the body center B is zero. Then, if leg 1 moves such that it possesses negative yaw angular momentum (e.g., when leg 1 moves from $\phi_1 = 0$ to $\phi_1 = \pi/2$), then the body starts yawing in a positive sense. When leg 1 is brought to rest, its yaw angular momentum reduces to zero. As a result, the body also comes to rest, ensuring that the total angular momentum is conserved.

An important feature of the yaw model is that the yaw inertia changes with leg configuration. For example, the yaw inertia is maximum when the legs are horizontal and is minimum when the legs are vertical. This variation of inertia with configuration influences yaw motion.

A simple strategy to achieve net yaw is to use interleaved leg motions. We will move each leg back and forth between extremes of 0 and $\pi/2$ rad. Each leg will dwell at the extreme for one second, and will take one second to transition between angles following a cubic spline. The result is a Lie bracket-inspired smoothed square wave, with the two legs $\pi/2$ rad out-of-phase (see Fig. 5). This sequence of leg motions yields a net yaw motion, as shown in Table II. This result can be confirmed by studying the table and thinking about the angular inertia of the system. Suppose the body yaw is ε_1 during interval $t = 0$ to $t = 1$, and is ε_2 during interval $t = 1$ to $t = 2$. The net yaw during the first two motion segments is different because the angular inertia varies, depending on whether the leg is stretched out or tucked in. This difference produces net yaw at the end of the motion sequence.

III. The Roll-Yaw model

Fig. 3 presents a set of roll-yaw body oscillations that produce RRRobot locomotion in the plane. In this section, we will find leg motions that produce

TABLE II

Incremental motion of the yaw model.

Time interval	$\phi_1(t)$	$\phi_2(t)$	Change in yaw
0–1	$0 \to \pi/2$	0	ε_1
1–2	$\pi/2$	$0 \to \pi/2$	$-\varepsilon_2$
2–3	$\pi/2 \to 0$	$\pi/2$	$-\varepsilon_2$
3–4	0	$\pi/2 \to 0$	ε_1
Net change in yaw			$2(\varepsilon_1 - \varepsilon_2)$

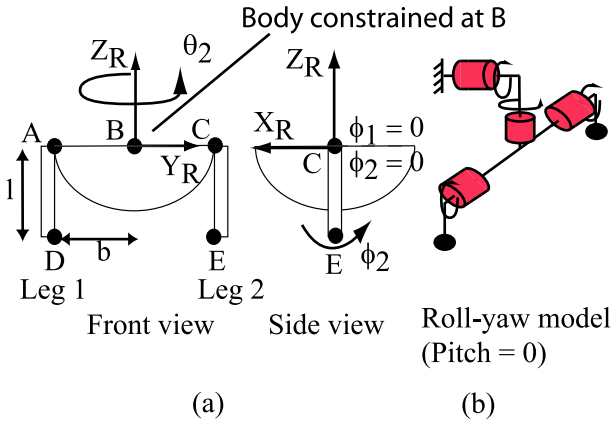

Fig. 6. (a) The simplified RRRobot model and (b) the roll-yaw model as a kinematic chain.

similar roll-yaw oscillations in a simplified version of RRRobot that can only roll and yaw.

A. The Roll-Yaw model details

The roll-yaw model (see Fig. 6) treated in this section is the same as the yaw model except for the additional roll freedom. Configuration is now given by $q = (\theta_1, \theta_2, \phi_1, \phi_2)^T \in \mathbb{R}^4$, where θ_1 and θ_2 represent the roll and yaw of the system. All body roll-yaw changes are small, but body pitch is constrained to be zero. The mass matrix of the system $M(q) \in \mathbb{R}^{4\times4}$ and the vector $C(q,\dot{q})\dot{q} \in \mathbb{R}^4$. Intuitively, we could follow a similar analysis procedure to that used in the yaw model to conclude that the robot can locally adjust $\theta_1, \theta_2, \phi_1$, and ϕ_2.

B. Roll-Yaw model simulations

To approximate RHex's specifications, we set: $m_m = 3$ kg, $m_l = 0.2$ kg, $l = 0.1$ m, and $b = 0.2$ m. Note that the roll inertia is minimal when the legs are stretched out and maximal when the legs are tucked in. This is opposite for the yaw inertia (see Fig. 7). We present three patterns of leg motions or *gaits* that produce roll-yaw motions. Gaits 1 and 2 are interleaved leg motions like in Fig. 5, and Gait 3 uses sinusoidal leg trajectories.

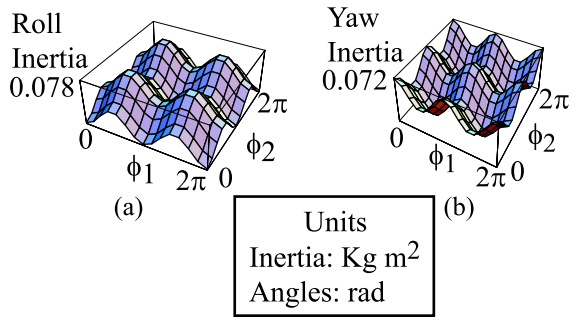

Fig. 7. Variation of the RRRobot (a) roll inertia and (b) yaw inertia with leg configuration.

Gait 1

In Gait 1, the legs move between angles of 0 and $\pi/4$ rad, and this produces predominantly positive yaw motion (see Fig. 8a). Swapping the order of leg motions gives body motion along the opposite direction; call this variation Gait 1′.

Gait 2

In Gait 2, the legs move between angles of $\pi/2$ and π rad, and this produces positive roll and negative yaw motion (see Fig. 8b). Call the variation obtained by swapping the order of leg motions Gait 2′.

In the absence of gravity, we can incrementally build up RRRobot's roll and yaw using many cycles of Gaits 1, 2, 1′, and 2′. Note that, by interleaving these gaits, we can create body attitude motions similar to the oscillations in Fig. 3 that cause RRRobot to translate in the XY-plane. (Although some leg motion is required to paste the gaits together, the net effect on roll and yaw is zero.)

Gait 3

Interleaving Gaits 1, 2, 1′, and 2′ produces roll-yaw oscillations in the roll-yaw model by incrementally building up large roll or yaw angles. But this is not practical for RHex or RRRobot, because, in the presence of gravity, the body would rock back to its equilibrium configuration. A more practical approach would be to use small continuous oscillations in roll and yaw.

Table III shows the parameters of Gait 3's sinusoidal leg trajectories of the form $a\sin(\omega t+\beta)+\gamma$. An envelope function ramps the legs from zero velocity to sinusoidal paths and ensures continuity in $(\dot{\phi}_1,\dot{\phi}_2)$ space. To eliminate any drift in roll and yaw due to the initial transients, we add damping of the

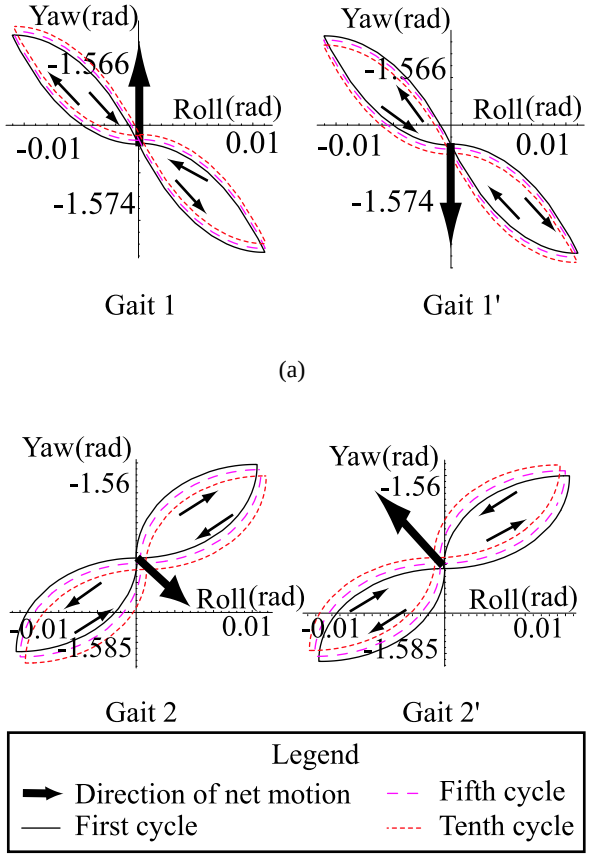

Fig. 8. Body attitude oscillations and net roll and yaw produced by (a) Gait 1 and Gait 1′ over ten cycles and (b) Gait 2 and Gait 2′ over ten cycles.

TABLE III
Gait 3 parameters.

	Leg 1	Leg 2
Amplitude a (rad)	$\pi/8$	$\pi/8$
Frequency ω (rad/s)	5	5
Phase β (rad)	0	$\pi/2$
Offset γ (rad)	0	$\pi/2$
Damping k	-1	-1

form $-k_i\dot{\theta}_i, k_i>0$ to the roll and yaw axis equations. Under Gait 3, the body settles down into a steady *rocking* pattern after initial transients (see Fig. 9). Note that this motion is similar to the roll-yaw attitude oscillations in Fig. 3 that produce RRRobot translation.

IV. Discussion

Suppose RRRobot has large pitch inertia so that pitch configuration changes are negligible compared to roll-yaw changes. Then, RRRobot is similar to

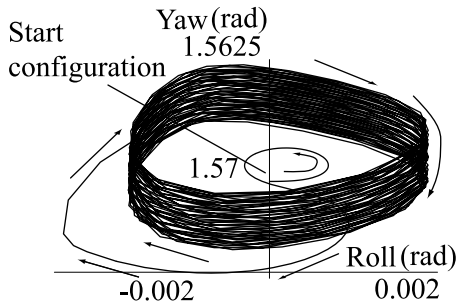

Fig. 9. Looping curves in roll-yaw space produced by Gait 3 over eighty cycles.

a unicycle, with yaw corresponding to unicycle direction, and body roll corresponding to forward motion. We can compute RRRobot XY-plane translation kinematically using:

$$\Delta X = \int v \sin\theta_2 dt, \quad \Delta Y = \int -v \cos\theta_2 dt, \qquad (4)$$

where $v = b\dot{\theta}_1$ is the body center velocity. We hypothesize that roll-yaw attitude oscillations produced using Gait 3 (see Section 3), when coupled with the nonholonomic contact constraints, will produce translation as in Fig. 3. More experiments are necessary to verify this on RRRobot and RHex. If true, eighty cycles of Gait 3 will produce a few millimeters of translation after about 100 secs (measured using (4)).

V. Conclusion

We have presented a set of models which, when superimposed, give a method of locomotion for high-centered legged robots using body attitude oscillations. We have used simplified dynamic models of a prototype robot to understand the interplay between leg motions and body attitude dynamics. Interesting future work includes developing fuller dynamic models of RRRobot locomotion and conducting experiments with RRRobot and RHex.

VI. Acknowledgment

This work was supported under NSF IIS 0082339, NSF IIS 0222875 and DARPA/ONR N00014-98-1-0747 contracts. We thank Devin Balkcom, George Kantor, and Uluc Saranli for insightful discussions on mechanical dynamic systems.

VII. References

[1] A. Bicchi, A. Balluchi, D. Prattichizzo, and A. Gorelli. Introducing the sphericle: an experimental testbed for research and teaching in nonholonomy. In *Proceedings of the IEEE International Conference on Robotics and Automation*, pages 2620–2625, 1997.

[2] C. Camicia, F. Conticelli, and A. Bicchi. Nonholonomic kinematics and dynamics of the sphericle. In *Proceedings of the IEEE International Conference on Intelligent Robots and Systems*, pages 805–810, 2000.

[3] W. Chow. Uber systeme von linearen partiel-len differentialgleichungen ester ordnung. *Math. Ann.*, 117:98–105, 1940.

[4] J. J. Craig. *Introduction to Robotics*. Addison Wesley, 1989.

[5] A. Lewis, J. Ostrowski, R. Murray, and J. Burdick. Nonholonomic mechanics and locomotion: The snakeboard example. In *Proceedings of the International Conference on Robotics and Automation*, pages 2391–2397, 1994.

[6] Z. Li and J. Canny. Motion of two rigid bodies with rolling constraint. *IEEE Transactions on Robotics and Automation*, 6(1):62–72, Feb. 1990.

[7] A. Marigo and A. Bicchi. Rolling bodies with regular surface: Controllability theory and applications. *IEEE Transactions on Automatic Control*, 45(9):1586–1599, Sept. 2000.

[8] R. M. Murray, Z. X. Li, and S. S. Sastry. *A Mathematical Introduction to Robotic Manipulation*. CRC Press, 1994.

[9] C. Rui, I. V. Kolmanovsky, and N. H. McClamroch. Nonlinear attitude and shape control of spacecraft with articulated appendages and reaction wheels. *IEEE Transactions on Automatic Control*, 45(8):1455–69, Aug. 2000.

[10] U. Saranli, M. Buehler, and D. E. Koditschek. Rhex: A simple and highly mobile hexapod robot. *International Journal of Robotics Research*, 20(7):616–631, July 2001.

[11] V. S. Varadarajan. *Lie Groups, Lie Algebras, and their Representations*. New York Springer Verlag, 1984.